J Porous Mater (2017) 24:437–442
DOI 10.1007/s10934-016-0278-9

Synthesis of MgAPO-31 nanocrystals via different heating methods and their catalytic performance in the hydroisomerization of *n*-decane

Jianwei Zhang[1] · Huimin Wu[1] · Aijuan Zhao[1] · Xuefeng Bai[1] · O. V. Kikhtyanin[2] · Wei Wu[1] · Linfei Xiao[1] · Xiaofang Su[1] · Rui Zhang[1]

Published online: 19 September 2016

Abstract MgAPO-31 molecular sieves substituted by different magnesium contents were synthesized using microwave irradiation (MW) and conventional electrical heating method, respectively. The bifunctional catalysts Pd/MgAPO-31 were prepared by the incipient wetness impregnation technique. The structure and acidity of MgAPO-31 were characterized by XRD, SEM, N_2 physical adsorption, FT-IR, and Py-IR. The catalytic performance of Pd/MgAPO-31 were tested in the hydroisomerization of *n*-decane, which was used as the probe-reaction, and the effect of heating method on acidity of MgAPO-31 and the catalytic performance of Pd/MgAPO-31 were investigated. The results showed that all of the MgAPO-31 samples with ATO topology structure were pure phase and high crystalline materials. The Mg(II) heteroatoms were confirmed to isomorphously substitute for the framework atoms of $AlPO_4$-31 molecular sieve. These Pd/MgAPO-31catalysts showed good catalytic performance for the hydroisomerization in the temperature range of 330–370 °C. The activity of Pd/MgAPO-31 in the hydroisomerization of *n*-decane and the selectivity for *i*-decanes were considered to depend on the crystal size and acidity of MgAPO-31.The highest selectivity for *i*-decanes was obtained over the catalyst Pd/0.05MgA31-MW prepared using the MW method.

Keywords MgAPO-31 molecular sieve · Isomorphous substitution · Microware irradiation · *n*-Decane · Hydroisomerization

1 Introduction

The hydroisomerization of *n*-alkanes to *iso*-alkanes is of considerable interest and has been intensively studied to improve the octane number of gasoline fractions and the low-temperature properties of diesel fuels [1, 2]. The isomerization of *n*-alkanes is generally performed over bifunctional catalysts containing metallic sites for hydrogenation/dehydrogenation and acid sites for skeletal isomerization via a carbenium mechanism. Catalysts based on molecular sieves with mono-dimensional non-intersecting and medium-pore channels have displayed high selectivity for the task [3, 4].

AlPO-n molecular sieves are microporous aluminophosphatematerials with an overall neutral framework without strong acidity [5]. AlPO-n molecular sieves can be transformed into catalytically useful materials by producing Brønsted acidity through the incorporation of other elements (Si, Mg, Mn, Co, Zn) to substitute for either P or Al + P to form SAPO-n or Al and eventually form MeAPO-n materials [6, 7]. The resulting sample has a negatively charged framework with ion-exchange capacity and Brønsted acidity once some of the framework atoms are substituted with other elements. Pt/MgAPO-11 with varying Mg contents synthesized using the hydrothermal method has proven to be an efficient catalyst in the hydroisomerization of *n*-dodecane. The Mg contents

✉ Wei Wu
wuwei@hlju.edu.cn

[1] International Joint Research Center of Catalytic Technology, Key Laboratory of Chemical Engineering Process and Technology for High-efficiency Conversion, College of Heilongjiang Province, School of Chemistry and Material Sciences, Heilongjiang University, Harbin 150080, Heilongjiang, China

[2] Research Institute of Inorganic Chemistry, RENTECH-UniCRE, Chempark Litvínov, Záluží, Litvínov 43670, Czech Republic

affected on the acidity, activity and isomer yield [8]. SAPO-31, with an ATO topology structure of a mono-dimensional cylindrical pore system and a 0.54 nm in pore diameter has been synthesized with different di-alkylamines. The catalysts prepared by Pd loading were active in the hydroconversion of *n*-decane and were highly selective towards isomerized products, reaching a maximum isomers yield of 80 % at an *n*-decane conversion of 90 % [9]. However, little information is available on the synthesis and application of MgAPO-31.

The most important benefit of applying microwave irradiation (MW) is that the synthesis mixtures can be rapidly heated to the desired temperature. Moreover, the direct energy transfer to the synthesis gels by MW allows for homogeneous heating and thus avoids the unwanted temperature gradients often encountered during conventional electrical (CE) heating. Compared to CE, the process of the hydrothermal synthesis of zeolites or aluminophosphate molecular sieves by MW has been attempted to increase the efficiency of the synthesis to achieve fast crystallization, high phase purity and narrow particle size distribution [10–13]. Therefore, MgAPO-31 synthesized by MW tends to exhibit different physico-chemical characteristics and catalytic performances.

Herein, a series of MgAPO-31 nanocrystals with different Mg contents were synthesized by MW and CE, and the heating method was correlated with the structure and acidity of the as-synthesized MgAPO-31. Pd/MgAPO-31 catalysts were used for the hydroisomerization of *n*-decane. The optimal heating method and Mg content were determined according to the relationship between the physic-chemical properties and catalytic performances.

2 Experimental

2.1 Synthesis of MgAPO-31 and preparation of the catalysts

Aluminum isopropoxide, ortho-phosphoric acid (85 %), $Mg(NO_3)_2{\cdot}6H_2O$ and di-n-butylamine (DBA) were used as the sources of aluminium, phosphorus, magnesium and template, respectively. MgAPO-31 molecular sieves were synthesized using a reactive gel with a molar composition of xMgO:yAl$_2$O$_3$:1.0P$_2$O$_5$:1.4DBA:40H$_2$O, where $x/2 + y = 1$, x was selected as 0.025 and 0.05. In all syntheses, the reactive gels were prepared as follows: ortho-phosphoric acid aqueous solution was mixed with aluminium isopropoxide and distilled water under stirring at room temperature. To this mixture, DBA was added followed by $Mg(NO_3)_2{\cdot}6H_2O$. For the synthesis of MgAPO-31 by MW, the experiments were performed in a microwave oven and were crystallized in an autoclave at 170 °C for 2 h using microwave irradiation heating. For the synthesis of MgAPO-31 by CE, the gels were transferred into a stainless-steel autoclave lined with polytetrafluorethylene(PTFE) and crystallized at 180 °C for 48 h. All solid products were washed with deionized water, dried overnight at 110 °C, and then calcined at 650 °C for 4 h to remove organic compounds. The samples synthesized by MW and CE were denoted xMgA31-MW and xMgA31-CE, respectively (where x stands for the Mg content). Bifunctional catalysts with Pd (0.5 wt%) loading were prepared by the impregnation of MgAPO-31 with the required amount of aqueous $Pd(NO_3)_2$ solution, which were denoted xMgA31-MW and xMgA31-CE.

2.2 Characterization

The synthesized samples were characterized by X-ray diffraction (XRD) on an X-ray diffractometer (Bruker, D8 Advance) fitted with Cu Kα radiation ($\lambda = 1.5406$ Å). The morphology was studied by a Hitachi S-4800 scanning electron microscope (SEM). The X-ray fluorescence spectrometry (XRF) was performed on a Bruker SRS3400 spectrometer to analyze the chemical compositions of the MgAPO-31 samples. The BET surface area was determined on an Autosorb-1-MP physical analyzer from Quantachrome. The infrared (IR) spectra were recorded on a FT-IR spectrometer (PESp-100). The pyridine-adsorbed infrared (Py-IR) spectra were recorded on Sp-100 Fourier transform infrared spectrometer from PE Company. Twenty milligrams of sample was pressed into a self-supported thin wafer and dehydrated at 350 °C for 2 h under a vacuum of 1.33×10^{-3} Pa, followed by the adsorption of pyridine vapor at 90 °C for 15 min. The spectra of adsorbed pyridine were recorded after evacuation for 1 h at 150 °C. The density of the Brønsted acid sites were calculated from the integrated area of the PyH^+ peaks using molar extinction coefficients of 1.67 cm/μmol, as determined by Emeis, respectively [14].

2.3 Hydroisomerization of *n*-decane

n-Decane isomerization was conducted in a continuously flowing tubular fixed-bed micro-reactor at 2.0 MPa. The catalysts were tested at a flow rate of hydrogen of 120 mL/min and a weight hourly space velocity of 2.5 h^{-1}. The reaction products were analyzed using a gas chromatograph (Agilent GC-6820) equipped with a flame ionization detector and an HP-1 capillary column.

3 Results and discussions

Figure 1 shows the XRD patterns of the MgAPO-31 molecular sieves samples with different contents of Mg synthesized by MW and CE, respectively. The crystallinity

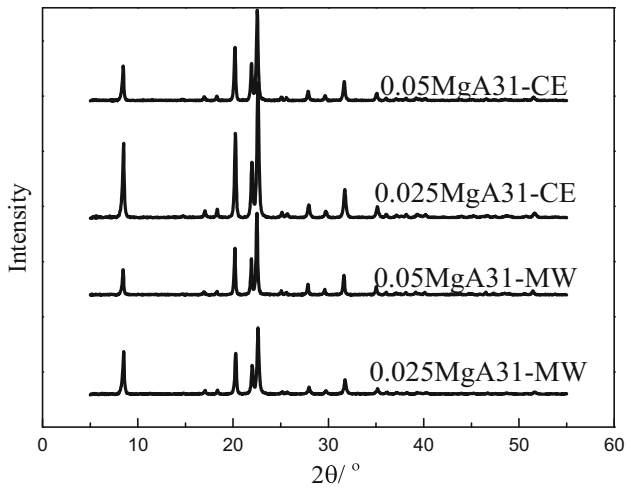

Fig. 1 XRD patterns of as-synthesized MgAPO-31 samples

of the MgAPO-31 samples estimated from the areas under the reflections in the diffraction angle range of $2\theta = 19° \sim 24°$ are shown in Table 1. Extraneous peaks were absent, and the spectra match those in the literature for ATO topology structures, indicating that all samples were free of impurities. The pure MgAPO-31 molecular sieve with high crystallinity was obtained by the CE method at a crystallization time of 48 h, whereas only 2 h was needed to achieve an equal crystallinity when the MW method was used, which demonstrated that the MW method significantly shortened the crystallization time compared with the CE method. One possible explanation was that the fast and instantaneous heating of MW made the depolymerization of the components in the reactive gel easier, and yielded more nuclei in a relatively short period to accelerate the crystallization of molecular sieves. Additionally, MW had the advantages of uniform heating and high efficiency, which could save a significant amount of time and significantly reduce energy consumption.

The crystallinity of samples synthesized by the CE method was higher than that of MW, due to the smaller crystal sizes of the samples synthesized by the MW method. As shown in Table 1, an increase in both the unit cell parameters and the unit cell volume was observed for the MgAPO-31 molecular sieves compared with $AlPO_4$-31, which indicates that Mg(II) was incorporated into the ATO framework, because Mg(II) has a larger radius [15].

The SEM images of the MgAPO-31 samples are presented in Fig. 2. An apparent difference in morphology was found between MgAPO-31 synthesized using the different heating methods. Broccoli-like shaped aggregates were shown on the MgA31-CE samples (Fig. 2a, b), while the MgA31-MW samples (Fig. 2c, d) possessed rod-like shaped aggregates, besides the aggregation degree of MgA31-MW samples was more compact.

The chemical composition of the samples determined by XRF is shown in Table 2. Compared to the *x*MgA31-CE samples, Mg content and Mg/P of *x*MgA31-MW samples were higher when the same gel composition had been used, which suggested that the MW heating method was conducive to Mg incorporation into the products.

Figure 3 and Table 3 depict the results of the adsorptive properties of the MgAPO-31 samples. The presence of an apparent hysteresis loop at $p/p_0 = 0.40 \sim 1.0$ was noted on the isotherms of the *x*MgA31-MW samples, which indicated that N_2 undergoes irreversible adsorption and desorption in the intercrystalline mesopore of the *x*MgA31-MW sample nanocrystals [16].

Larger mesopore volume and external surface area for the *x*MgA31-MW samples were observed. The aggregated *x*MgA31-MW nanocrystallites with relatively smaller crystal size favored the formation of more mesopores. In addition, defects caused by isomorphous substitution of Mg led to the formation of intercrystalline mesopores in the samples synthesized using the MW method with a relatively short crystallization time.

The FT-IR spectra and the corresponding datas of the MgAPO-31 molecular sieves are shown in Fig. 4a and Table 4. A shift in all T-O frequencies to lower wavenumbers for the MgAPO-31 samples compared to $AlPO_4$-31 was observed which confirmed the isomorphous substitution of Mg into the molecular sieves framework [17, 18].

Table 1 Crystallographic data of MgAPO-31 molecular sieve samples

Sample	Unit cell parameters			Relative crystallinity[a](%)
	A/Å	C/Å	V/Å^3	
$AlPO_4$-31	20.840	5.007	1883.30	99
0.025MgA31-CE	20.869	5.032	1897.90	95
0.025MgA31-MW	20.877	5.026	1897.10	93
0.05MgA31-CE	20.857	5.028	1894.22	100
0.05MgA31-MW	20.889	5.026	1899.29	91

[a] The relative crystallinity of the as-synthesized MgAPO-31samples

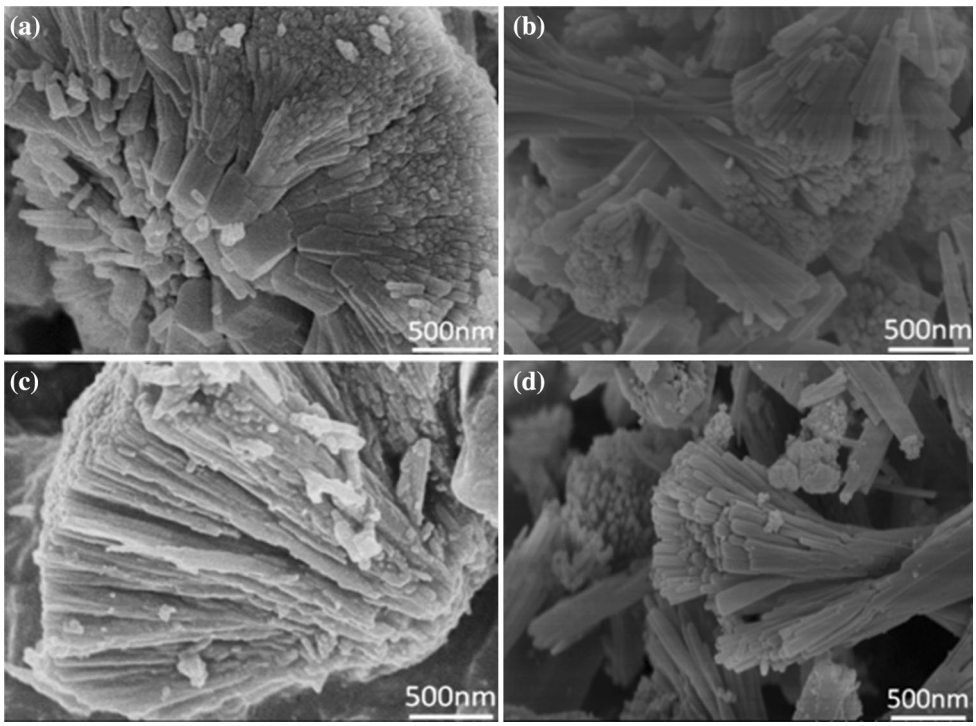

Fig. 2 SEM images of MgAPO-31 molecular sieves samples. **a** 0.025MgA31-CE, **b** 0.05MgA31-CE, **c** 0.025MgA31-MW, **d** 0.05MgA31-MW

Table 2 Chemical compositions of MgAPO-31 samples

Sample	Composition of the products
0.025MgA31-CE	$Mg_{0.005}Al_{0.532}P_{0.478}O_2$
0.025MgA31-MW	$Mg_{0.006}Al_{0.527}P_{0.481}O_2$
0.05MgA31-CE	$Mg_{0.013}Al_{0.515}P_{0.486}O_2$
0.05MgA31-MW	$Mg_{0.015}Al_{0.527}P_{0.478}O_2$

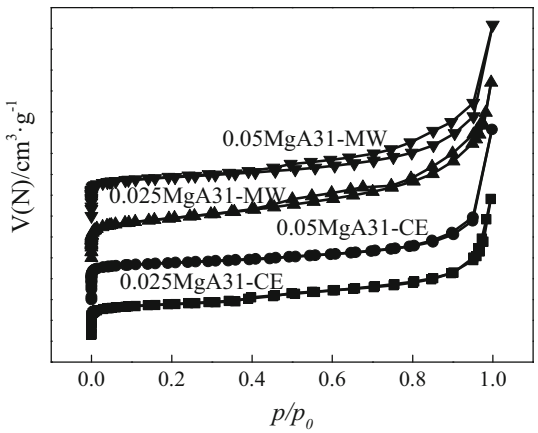

Fig. 3 N_2 adsorption–desorption isotherm of MgAPO-31 samples

A comparison of the IR spectra of adsorbed pyridine recorded for MgAPO-31 samples at 150 °C is presented in Fig. 4b, and the Brønsted acid sites density of MgAPO-31 samples is showed in Table 5. The results indicated that the bands at $\sim$1545 cm^{-1} corresponded to the adsorption of pyridine molecules on the Brønsted acid sites.

The number of total Brønsted acid sites determined by Py adsorption was higher in the *x*MgA31-CE samples with the same initial reaction gel composition due to the slower crystallization rate by CE heating method, therefore, more Mg was incorporated into the framework by isomorphous substitution to form acid sites compared to the *x*MgA31-MW samples. The number of total Brønsted acid sites is in the following order: 0.05MgA31-CE > 0.05MgA31-MW > 0.025MgA31-CE > 0.025MgA31-MW.

The dispersion of Pd, accessible Pd active sites (C_{Pd}), total Brønsted acid sites (C_{H+}) and C_{Pd}/C_{H+} ratio of the bifunctional catalysts Pd/MgAPO-31 catalysts are listed in Table 6, which indicated that Brønsted acid sites had declined after preparation of bifunctional catalysts, higher Pd dispersion and C_{Pd} were obtained on the samples prepared by CE heating method which was consistent with the more C_{H+}.

Figure 5a shows the *n*-decane conversion as a function of temperature over different bifunctional catalysts Pd/MgAPO-31. An increase in the *n*-decane conversion was obtained for all catalysts with increasing reaction temperature. The metal sites was sufficiently (larger C_{Pd}/C_{H+} ratio) for hydro-/dehydrogenating function, therefore activity of the bifunctional catalysts may be associated with the concentrations of total Brønsted acid sites in the samples, therefore Pd/*x*MgA31-CE prepared with the same initial gel composition exhibited higher catalytic activity compared with the Pd/*x*MgA31-MW. The activity of the

Table 3 BET surface area and pore volume of MgAPO-31 samples

Sample	Surface area (m^2/g)			Pore volume (cm^3/g)		
	BET[a]	Micropore[b]	External	Total[c]	Micropore[b]	Mesopore
0.025MgA31-CE	168	119	49	0.265	0.043	0.222
0.025MgA31-MW	168	101	67	0.326	0.040	0.286
0.05MgA31-CE	168	116	52	0.316	0.046	0.270
0.05MgA31-MW	174	106	68	0.355	0.042	0.313

[a] BET method

[b] t-plot method

[c] Volume adsorbed at $p/p_0 = 0.99$

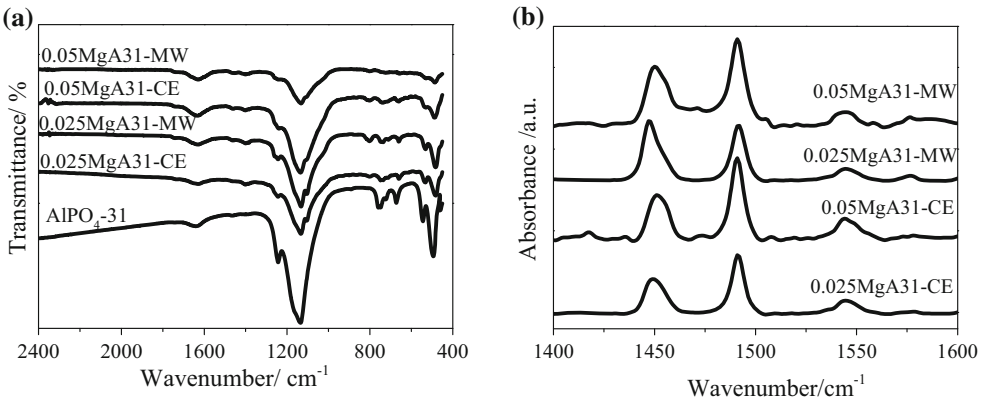

Fig. 4 FT-IR spectra of $AlPO_4$-31 and MgAPO-31 samples (**a**) and Py-IR spectra of MgAPO-31 samples recorded at 150 °C (**b**)

Table 4 The wave numbers observed in FT-IR spectra for $AlPO_4$-31 and MgAPO-31 samples

Sample	Wave number/cm^{-1}				
	A	B	C	D	E
$AlPO_4$-31	1136	760	672	544	494
0.025MgA31-CE	1133	748	658	531	483
0.025MgA31-MW	1132	748	658	531	483
0.05MgA31-CE	1134	735	658	531	489
0.05MgA31-MW	1131	733	654	527	485

[a] Asymmetric stretching vibration of the T-O-T tetrahedron

[b] Symmetric stretching vibration of the T-O-T

[c, d] Vibration of the silicoaluminophosphates building units

[e] Bending vibration of T-O-T(T = Al, P, Mg)

Table 5 Acidity of MgAPO-31 samples

Sample	Total Brønsted acid sites (μmol/g)
0.025MgA31-CE	25.6
0.025MgA31-MW	13.7
0.05MgA31-CE	29.7
0.05MgA31-MW	27.7

Density of Brønsted acid determined by of pyridine adsorbed FT-IR at 150 °C

catalysts was in the following order: Pd/0.05MgA31-CE > Pd/0.05MgA31-MW > Pd/0.025MgA31-CE > Pd/0.025MgA31-MW.

The bifunctional catalysts based on the *x*MgA31-MW samples showed higher selectivity for *i*-decane than *x*MgA31-CE samples with the same Mg content in initial gel. Compared with other catalysts, Pd/0.05MgA31-MW showed the highest isomerization selectivity of 95.4 % for *i*-decanes at an *n*-decane conversion of 86.8 %. This is because of the MW method promoted the depolymerization of the components in the reactive gel easier, and more nuclei were obtained in a relatively short period, resulting in smaller particles, which formed intercrystalline mesoporosity and enhanced the improved diffusion of branched intermediates and *i*-decanes from the channels of the molecular sieves, and inhibited their cracking.

Pd/0.025MgA31-CE and Pd/0.025MgA31-MW showed decreased selectivity for *i*-decanes at the same *n*-decane conversion, due to the necessity to apply a higher temperature over these catalysts with a lower amount of total Brønsted acid sites, thus intensifying the cracking of branched-isomers.

Table 6 Results of H_2 chemisorption over 0.5 wt% Pd/MgAPO-31

Sample	Pd dispersion (%)	C_{Pd} (μmol/g)[a]	C_{H+}(μmol/g)[b]	C_{Pd}/C_{H+}
Pd/0.025MgA31-CE	20.3	9.5	13.2	0.72
Pd/0.025MgA31-MW	17.8	8.4	12.2	0.69
Pd/0.05MgA31-CE	20.6	9.7	19.7	0.49
Pd/0.05MgA31-MW	17.9	8.4	17.7	0.47

[a] Concentrations of accessible Pd atoms

[b] Concentrations of Brønsted acid sites of bifunctional catalysts

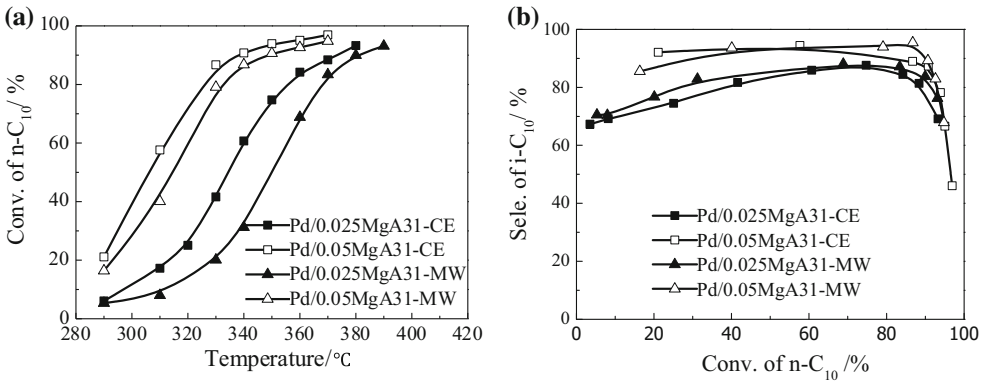

Fig. 5 *n*-decane conversion *vs.* temperature (**a**) and isomerization selectivity for *i*-decanes versus *n*-decane conversion (**b**) over Pd/MgAPO-31 catalysts

4 Conclusions

In summary, MgAPO-31 molecular sieves nanocrystals were successfully synthesized by both conventional the conversional electrical heating (CE) method with the crystallization of 48 h and the microwave irradiation heating (MW) method with a shorter crystallization time of 2 h. Mg(II) heteroatoms were confirmed to isomorphously substitute for the atoms of the $AlPO_4$-31 framework under the suitable gel composition. The properties of the samples obtained by the CE and MW methods possessed different crystallinity, crystalline size, acidity and catalytic performance. The Pd/0.05MgA31-CE catalysts demonstrated the highest activity in the *n*-decane hydroisomerization due to larger amount of Brønsted acid sites. The Pd/0.05MgA31-MW showed the highest selectivity to *i*-decanes in the *n*-decane hydroisomerization owing to its suitable amount of Brønsted acid sites and increased mesoporosity, which improved the diffusion of branched carbenium intermediates.

Acknowledgments Financially supported by Program of International S&T cooperation (2013DFR40570) and National Natural Science Foundation of China (No. 21411130188, 21276067).

References

1. K.C. Park, S.K. Ihm, Appl. Catal. A Gen. **203**, 201 (2000)
2. K.G. Fang, W. Wei, J. Ren, Y.H. Sun, Catal. Lett. **93**, 235 (2004)
3. L.B. Galperin, Appl. Catal. A. Gen. **209**, 257 (2001)
4. P. Meriaudeau, V.A. Tuan, V.T. Ngheim, C. Naccahe, G. Sapaly, Catal. Today **49**, 285 (1999)
5. J. Li, G. Li, C. Xi, Chem. Res. Chin. U. **20**, 131 (2004)
6. S.H. Jhung, T. Jin, Y.H. Kim, Microporous Mesoporous Mater. **109**, 58 (2008)
7. W. Fang, R. Li, T. Dou, Microporous Mesoporous Mater. **84**, 116 (2005)
8. Y. Xiaomei, X. Zhusheng, T. Zhijian, Catal. Lett. **109**, 139 (2006)
9. J. Yang, O.V. Kikhtyanin, W. Wu, Microporous Mesoporous Mater. **150**, 14 (2012)
10. S.H. Jhung, J.S. Chang, J.S. Hwang, S.E. Park, Microporous Mesoporous Mater. **64**, 33 (2003)
11. K. Utchariyajit, S. Wongkasemjit, Microporous Mesoporous Mater. **135**, 116 (2010)
12. S.C. Laha, G. Kamalakar, R. Glser, Microporous Mesoporous Mater. **90**, 45 (2006)
13. M. Gharibeh, G.A. Tompsett, W.C. Conner, Top. Catal. **49**, 157 (2008)
14. C.A. Emies, J. Catal. **141**, 347 (1993)
15. L. Feng, X. Qi, L. Zheng, Chin. J. Catal. **30**, 340 (2009)
16. J.C. Groen, L.A. Peffer, J. Perez-Ramirez, Microporous Mesoporous Mater. **60**, 1 (2003)
17. J. Li, Y. Guo, G. Li, J. Chen, Microporous Mesoporous Mater. **79**, 79 (2005)
18. S. Hui, Y. Jianfeng, K. Xuebin, Z. Lixiong, X. Nanping, Mater. Res. Bull. **44**, 956 (2009)